E R D K U N D E
Band 57, Heft 2 B.o.s.s Druck und Medien, Kleve Juni 2003

A CASE STUDY ON RAINFALL DYNAMICS DURING EL NIÑO/LA NIÑA 1997/99 IN ECUADOR AND SURROUNDING AREAS AS INFERRED FROM GOES-8 AND TRMM-PR OBSERVATIONS

With 8 figures and 3 tables

JÖRG BENDIX, STEFAN GÄMMERLER, CHRISTOPH REUDENBACH and ASTRID BENDIX

Zusammenfassung: Niederschlagsdynamik während El Niño/La Niña 1997/99 in Ecuador und benachbarten Gebieten – Eine Fallstudie auf der Basis von GOES-8- und TRMM-PR-Daten

Das Klimaphänomen El Niño/La Niña (EN/LN) verursacht in den trockenen Küstenregionen Südecuadors und Nordperus (El Niño) bzw. an der andinen Ostabdachung (La Niña) extreme Starkniederschläge, Überflutungen und eine Vielzahl ökonomischer Schäden. Da die raum-zeitliche Niederschlagsverteilung sowie die Niederschlagsgenese während Super-Ereignissen nicht abschließend geklärt ist, wurde die Starkniederschlagsdynamik für die betroffenen Gebiete in Ecuador und Nordperu während des stärksten Super El Niño des vergangenen Jahrhunderts (1997/98) sowie dem nachfolgenden La Niña-Ereignis analysiert. Die Untersuchungen basieren auf Bildsequenzen von GOES-8- und Radardaten der TRMM-Mission (PR-Sensor). Zur Erfassung der raum-zeitlichen Niederschlagsverteilung sowie der Zirkulationsmuster wurden aus den GOES-Daten Niederschlagskarten mit Hilfe der Enhanced Convective Stratiform Technique (ECST) und Cloud Motion Wind (CMW)-Karten berechnet. Aus den Untersuchungen ergibt sich, dass die raum-zeitliche Niederschlagsdynamik während des Super El Niño (1997/98) ähnlich wie bei einem normalen El Niño (1991/92) verläuft. Allerdings ist die Gesamtniederschlagsmenge signifikant erhöht. Überströmungsvorgänge von Cirrenresten aus dem Amazonastiefland über die Anden können durch die Analyse der TRMM-PR-Daten im Zusammenhang mit den CMW-Karten eindeutig belegt werden. Im Vergleich zu El Niño ist für ein La Niña-Ereignis eine inverse Niederschlagsverteilung charakteristisch. Für La Niña 1999 wird die raum-zeitliche Niederschlagsdynamik mit den zugehörigen Zirkulationsmustern erläutert.

Summary: El Niño and La Niña (EN/LN) events cause heavy precipitation, floods and various economical losses in the normally extreme dry coastal areas of southern Ecuador and northern Peru (El Niño) as well as at the eastern-Andean slopes (La Niña). Due to the fact that the spatio-temporal rainfall distribution and rainfall formation during "super events" is still not definitely known today, an analysis of heavy precipitation dynamics during the strongest Super El Niño of the last century (1997/98) for Ecuador and northern Peru and the following La Niña (1999) event is presented. The investigation is based on half-hourly time series of GOES-8 and additional radar data onboard the TRMM platform (PR-Sensor). The Enhanced Convective Stratiform Technique (ECST) was applied to compute precipitation maps in order to examine the spatio-temporal rainfall distribution. Additionally, Cloud Motion Winds (CMW) are extracted from the GOES-8 data in order to investigate the related circulation pattern. It has been proven that the spatio-temporal dynamics of heavy precipitation during the Super El Niño 1997/98 reveals the same mechanisms as during a normal El Niño (1991/92). However, the rainfall amount is significantly increased. Evidence for clear spill-over effects of cirrus remainders from the Amazon region on the rainfall formation in the coastal lowlands could be found by means of TRMM-PR data and CMW's. The La Niña situation (1999) is typified by an inverse spatial distribution of rainfields. The specific La Niña weather situation with its typical circulation patterns is outlined.

1 Introduction

The El Niño (EN) phenomenon is the most common climate anomaly which occurs quasi-periodically in the tropical Pacific. The central area in the eastern Pacific which is strongly affected during El Niño events is the coastal part and the western Andean slopes of Ecuador and northern Peru (Sechura Desert). The time-series analysis of precipitation data shows that the intensity and re-occurrence of EN increased at the end of the last century (Fig. 1 and BENDIX et al. 2000).

Especially the extreme events (so called Super El Niños) cause heavy precipitation, floods and economical losses as well as an increased frequency of diseases like dengue fever or malaria in the coastal areas of Ecuador and northern Peru. For Ecuador, the 1997/98 EN was the strongest event of the last century, exceeding the last Super EN of 1982/83 (GASPARRI et al. 1999; BENDIX 2000b). The infra-structural damages of Ecuador alone amount to more than 200 Mio. US$ and occur mainly in the five coastal provinces (El Oro, Esmeraldas, Guayas, Los Rios, Manabi). Losses in agriculture are quantified to 104.7 Mio. US$ (Tab. 1). The poor population (landless agricultural workers) suffers from the greatest financial losses and is also mostly affected by the increase of water-borne diseases. Only shrimp production profits from increased sea surface temperatures in the coastal waters.

However, the coastal provinces are not affected equally (Tab. 2). The poorer provinces whose economy is dominated by the agricultural sector reveal severe damages and losses whereas the northern and southernmost provinces are characterised by weaker impacts.

Because the spatial differentiation in vulnerability is especially a result of the spatial structure of heavy rainfall and subsequent flooding, a detailed knowledge about the spatio-temporal dynamics of heavy rainfall during EN events e. g. for protection measures is required. On the other hand, strong La Niña (LN) events which often succeed Super ENs are also of interest for the current study because they are generally most likely to produce above-average precipitation at the eastern-Andean slopes of Ecuador (VUILLE et al. 2000; BENDIX a. RAFIQPOOR 2001). This also leads to damages such as severe landslides. However, the current knowledge about spatio-temporal LN effects in Ecuador is rather poor (CORNEJO a. DE GRUNAUER 2002).

The spatial distribution of rainfall has been investigated for EN events of the last decades in several investigations. These studies have proven that anomalous heavy precipitation is mainly concentrated in the coastal plains up to an altitude of ~1,800 m asl (e. g. BENDIX 2000b). In general, positive SST anomalies off the coast of Ecuador, the resulting high amount of precipitable water in the atmosphere as well as the anomalous atmospheric circulation pattern in the tropical Pacific are the basis of the formation of strong positive precipitation anomalies (e. g. ZHOU et al. 1996; VAN OLDENBORGH 2000). However, the local and regional dynamics of heavy precipitation in Ecuador and northern Peru is only considered in a few studies (SCHÜTTE 1968; HOREL a. CORNEJO-GARRIDO 1986; GOLDBERG et al. 1987; CAVIEDES a. ENDLICHER 1989; ROSSEL et al. 1998; BENDIX et al. 2000), and hence, a lack of spatio-temporal information on heavy precipitation on the local and regional scale still exists today. Only one analysis concerning the normal EN 1991/92 covers the whole area of Ecuador and northern Peru (BENDIX 2000a).

The results of some of these studies (especially EN 1991/92) point out specific mechanisms which are responsible for the formation of heavy precipitation:

1 – An increase in convection originated from an intensified land-sea breeze system which is sometimes coupled with convection due to thermal up-slope winds on the western Andean slopes. Precipitation shows a patchy structure and a clear diurnal cycle with a heavy rainfall maximum along the sea-breeze front which is located approximately ±50 km inland, sometimes associated with the first coastal Cordillera (e. g. in the area of Chone). Heavy precipitation in the coastal plains occurs during late afternoon and evening, in comparison to nocturnal precipitation over the coastal waters which is induced by the land-breeze system.

2 – Heavy rainfall which covers the whole coastal plains as well as the coastal waters without any distinct diurnal cycle and persisting several days. Precipitation is related to mesoscale convective complexes (MCC) which predominantly form in coastal areas with anomalous high SST but strong spatial SST gradients. The MCC-borne rainfall is frequently shifted to the coastal plains by anomalous westerlies.

3 – During phases of convection in the Amazon in combination with well-established easterlies in the mid and upper troposphere, cirrus remainders spill over the Andes, producing deep convection and heavy rainfall due to seeding effects in the area of initial convection from the coupled sea-breeze/up-slope thermal systems.

Due to the fact that spatio-temporal dynamics on heavy rainfall in Ecuador and northern Peru has not yet been investigated for Super El Niño and La Niña events with spatial data sets, it is the aim of the current study to examine the spatial distribution as well as the formation of heavy precipitation during EN 97/98 by means of satellite data. The second part of the analysis focuses on heavy rainfall dynamics during a strong La Niña event (LN 1999). This is the first cold event which is examined for Ecuador and adjacent areas with the comprehensive methodology which is presented in the next chapter.

2 Study area, data and methods

The central study area covers Ecuador and the northern part of Peru, which is characterised by normally dry conditions in the coastal lowlands (Sechura desert), between 82.5°W 1°N and 75°W 6°S (Fig. 1). The region of interest is subdivided into the coastal plains, the Andean highlands including the eastern and the western cordillera and the inter-Andean basins as well as parts of the Amazon region. The course of precipitation in the coastal plains, the inter-Andean basins and parts of the Ecuadorian Amazon region during a normal year is generally characterised by two rainy seasons in March/April and October/November (BENDIX a. LAUER 1992). However, in the more arid southern parts of Ecuador and in northern Peru (Sechura), only one short rainy season with a peak in March occurs. Additionally, a special regime exists on the eastern Andean slopes between approximately 1,000 and 3,200 m asl which is characterised by one rainy season centred in July (for further explanations of this effect

refer to BENDIX and LAUER, 1992). Precipitation during El Niño events generally exceeds many times the amount of rain of a normal rainy season (maximum in March): at individual meteorological stations measurements vary from approximately +1,000% of the average during a normal El Niño event up to +7,900% during Super El Niño events. Additionally, the normally short rainy season in the southernmost parts of the study area is temporally extended (BENDIX 2000b).

Investigations of rainfall dynamics in the current study are mainly performed by means of satellite data. GOES-8 channel 3 and 4 data (#3: WV 6.47–7.02 μm, #4: IR 10.2–11.2 μm) have been used for rainfall retrieval and the determination of cloud motion winds during EN/LN 1997/99. For further details of the GOES system refer to MENZEL and PURDOM (1994). 21 days (Tab. 3) of maximum precipitation in Ecuador and northern Peru have been selected by the inspection of raingauge data. Hence, more than 1,000 slots mostly with half-hourly temporal resolution are used in the current study. In order to address the question of spill-over effects from the Andes and to investigate 3D-rainfall dynamics, TRMM (Tropical Rainfall Measuring Mission)-PR data (Precipitation Radar) were evaluated. A comprehensive overview of the TRMM mission and the sensor package is given by KUMMEROW et al. (1998). 142 TRMM orbits between December 1997 and March 1998 (EN) as well as January-April 1999 (LN) were selected. The study makes use of the PR product 2A25 which, among others, consists of vertical rain rate profiles and 2D-fields of near surface rainfall. This product has already been successfully used for the investigation of the 3D-distribution of topical rainfall in other areas

Table 1: Profits and losses in Ecuadorian agriculture during EN 1997/98 (Data from GASPARRI et al. 1999)

Gewinne und Verluste in der ecuadorianischen Landwirtschaft während El Niño 1997/98

	Farmer (landowner)	Agricultural worker	Traders	Shrimp farmers	Fishery	Total
Mio US$	–44.1	–73.9	–49	68	–5.7	–104.7

Table 2: General losses in the coastal provinces of Ecuador during EN 1997/98 in percent of the average annual per capita income (Data from GASPARRI et al. 1999)

Ökonomische Verluste der ecuadorianischen Küstenprovinzen während EN 1997/98 in Prozent des mittleren jährlichen Pro-Kopf-Einkommens

	El Oro	Guayas	Los Rios	Manabi	Esmeraldas
Income [US$]	962	666	608	593	615
Farmers [%] (landowner)	0.6	2.1	4.8	2.2	0.2
Agricultural Worker [%]	2.7	8.7	14.3	4.7	1.1
Traders [%]	0.8	3	6.1	2.4	0.2

Table 3: Selected days of maximum precipitation during El Niño – La Niña 1997–1999

Ausgewählte Untersuchungstage mit maximalen Niederschlägen für El Niño – La Niña 1997–1999

El Niño 1997/98	La Niña 1999
97/11/23	99/01/08 99/01/17 99/01/23
98/01/12 98/01/24	99/02/02 99/02/24
98/02/08 98/02/17 98/02/26	99/03/07 99/03/20 99/03/22 99/03/31
98/03/05 98/03/09 98/03/16 98/03/22	99/04/13
98/03/23	

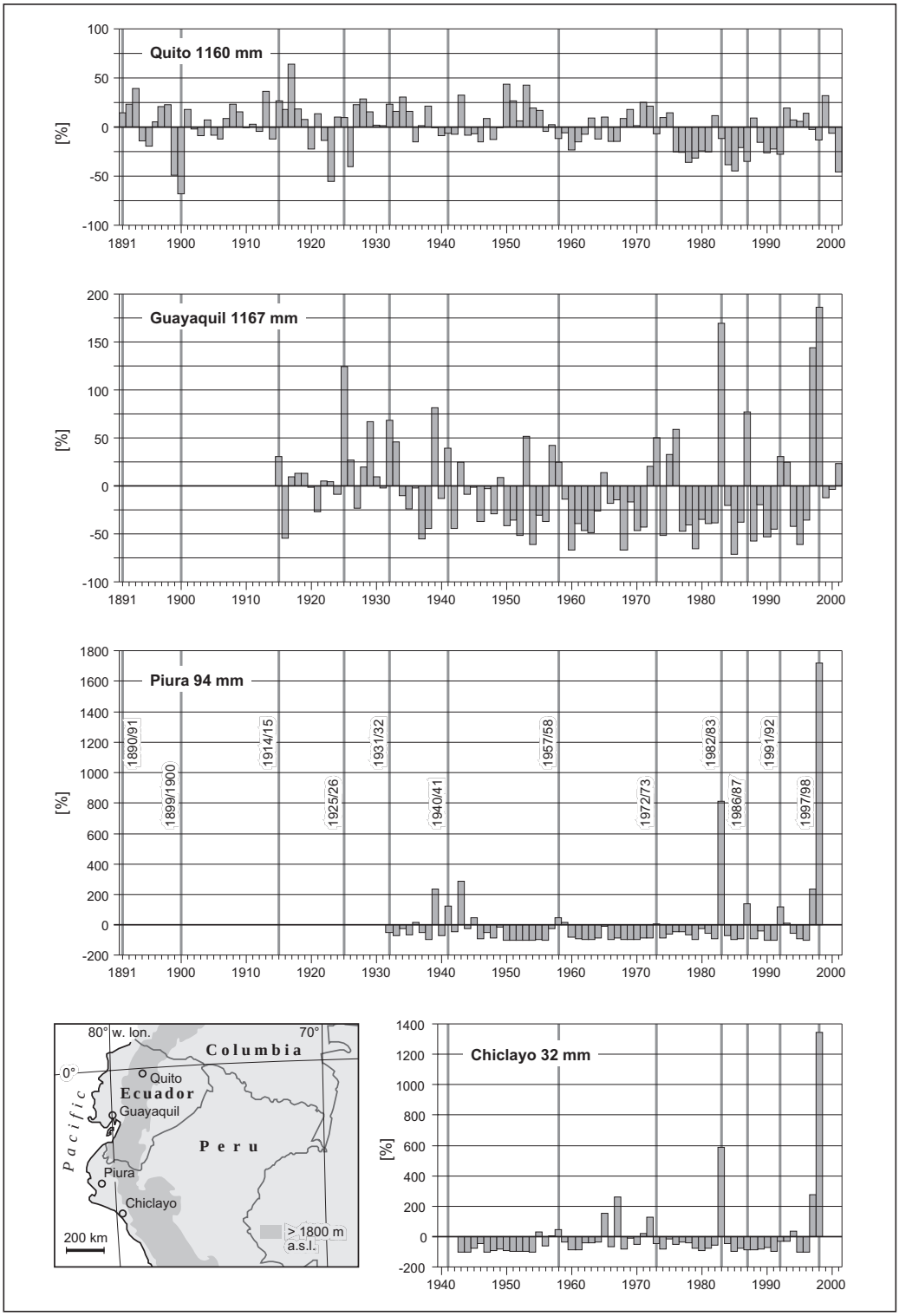

Fig. 1: Time series of relative deviations from average precipitation at selected stations in Ecuador and northern Peru (Data: INAMHI, SENAMHI).

Zeitreihe der relativen Abweichung vom Niederschlagsmittel für ausgewählte Stationen in Ecuador und Nordperu

(e. g. NIRALA a. CRACKNELL 2002). For details of the 2A25 retrieval algorithm refer to IGUCHI et al. (2000). Ancillary data sets are raingauge oberservations of the national weather services (INAMHI Ecuador, SENAMHI Peru), radiosoundings from the stations Galapagos (Ecuador) and Porto Velho, Manaus and Alta Floresta (Brazil), as well as a Digital Elevation Model (USGS GTOPO30).

The complete methodology of the current study is presented in figure 2. The rainfall retrieval for the computation of precipitation maps from GOES-8 data was realised by using the Enhanced Convective Stratiform Technique (ECST) (REUDENBACH et al. 2001). The ECST algorithm was adjusted both to the GOES sensor characteristics and to the regional rainfall dynamics. The extraction of cloud motion winds (CMW) for three atmospheric levels (lower, mid and upper troposphere) from sequences of GOES-8 images is performed by means of the cross-correlation technique (SCHMETZ et al. 1993; BENDIX a. BENDIX 1998). NOAA AVHRR-based MCSST-data (Multichannel Sea Surface Temperatures, not shown in this paper) are additionally used for interpretation purposes (MCCLAIN et al. 1985).

3 The Super El Niño 1997/98

3.1 Spatio-temporal rainfall dynamics

The analysis of precipitation extension for the Super EN 1997/98 reveals spatio-temporal structures which are also observed during previous normal events (Fig. 3).

The map of total precipitation shows maximum values in the coastal areas of Ecuador and northern Peru (up to ~1,800 m asl) extending to the eastern Pacific between the equator and 5°N. Only small patches in the Amazon area reach the same amounts as the rainfall maximum over the coastal waters. The maximum between the Galapagos Islands and the Ecuadorian coast is related to positive SST anomalies and originated mostly from MCCs. The inter-Andean

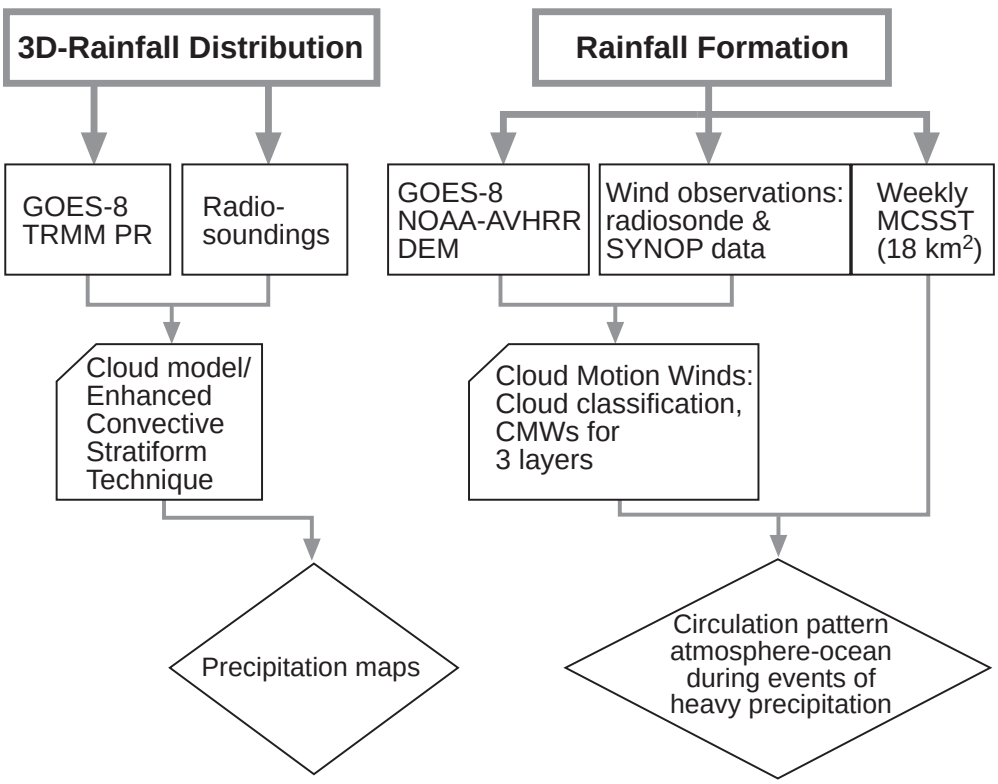

Fig. 2: Methodology of the current investigation
Methodik

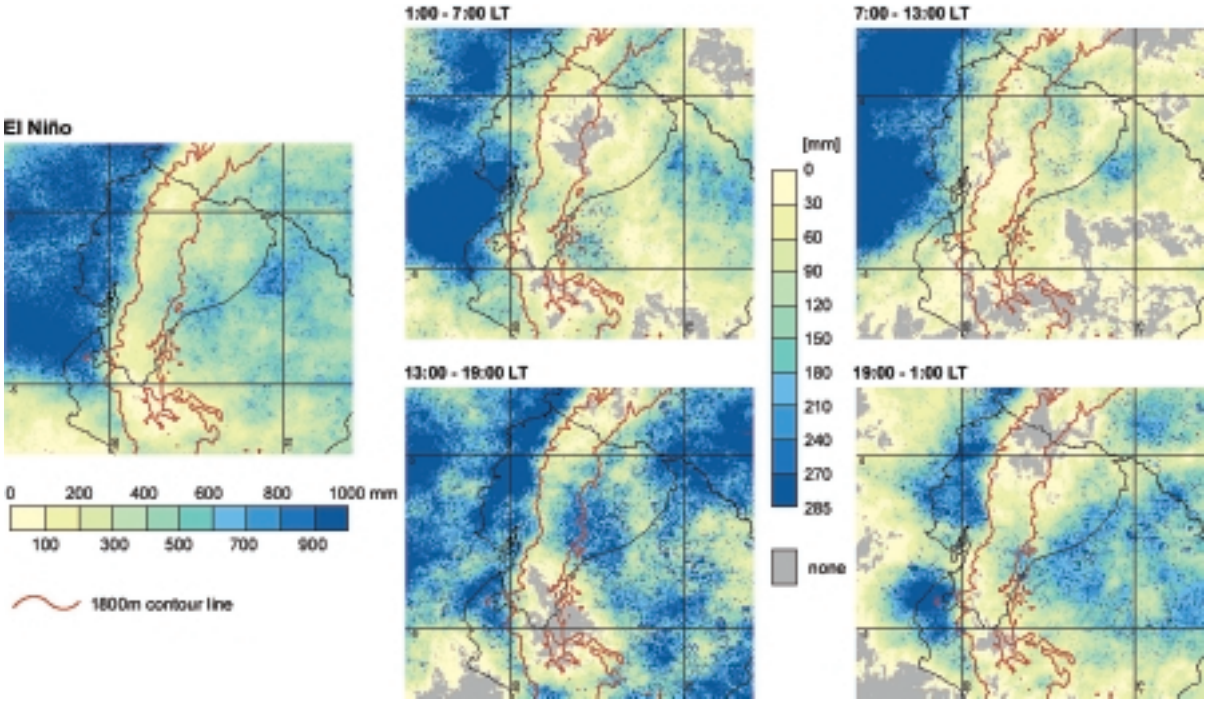

Fig. 3: Precipitation (ECST) during El Niño 1997/98 (11 days) (left) and diurnal course (right), LT = UTC – 5 h
Niederschlagsverteilung (ECST) während EN 1997/98 (11 Tage) (links) und Tageszeitengang (rechts), LT = UTC – 5 h

basins are relatively dry, no overall effect of anomalous rainfall above average is detected. The area south of the equator becomes dryer with increasing latitude.

The temporal distribution of precipitation over 24h shows a clear diurnal course of precipitation (Fig. 3, right). Maximum convection and rainfall over land is generally observed between 13:00 and 1:00 LT whereas in the night and early hours of the morning, maximum precipitation dominates over the coastal waters. This spatio-temporal pattern points to rainfall formation partially as a result of mesoscale thermal systems which was also observed during the normal event of 1991/92 (BENDIX 2000a). Rainfall from 1:00 to 7:00 LT is especially increased in the coastal waters. One maximum can be clearly detected around the Gulf of Guayaquil area which is an indicator for a well-developed land-breeze phenomenon. The coastal configuration of the Gulf promotes the confluence of the land-breeze from three directions. The result is deep convection with heavy rainfall, especially in combination with relatively warm water and the closest proximity to the eastern Andean slopes with their nocturnal down-slope winds. The spatial extended rainfields over the coastal waters are slightly shifted towards the Pacific between 7:00 and 13:00 LT. The daytime cycle starts between 13:00 and 19:00 LT. Maximum rainfall is observed in the Amazon region as well as in the coastal plains of Ecuador and northern Peru. However, there is a small, coast-parallel line of reduced precipitation which separates the rainfall maximum off the coast and that of the coastal plain. This line clearly indicates the divergence area from the back-flowing branch of the sea-breeze system. The great importance of the sea-breeze system on the spatial structure of EN precipitation is also observed between 19:00 and 1:00 LT. Only the coastal plains show significantly enhanced precipitation, especially around the Gulf of Guayaquil while the Gulf area itself is characterised by reduced values. Again, this is due to the coastal configuration which now favours strong divergence over the Gulf due to the divergent outflow of the sea-breeze into three sectors.

Although the mechanism of rainfall dynamics during EN 1997/98 is similar to a normal EN, the total amount of precipitation during EN 1997/98 is significantly higher (for comparison purposes refer to BENDIX, 2000a).

3.2 Analysis of single events

During the previous study of the 1991/92 normal EN, spill-over activities of cirrus remainders from the Amazon to the coastal lowlands seemed to play a key role in the intensification of rainfall formation which is originated by the land-sea-breeze phenomenon (BENDIX 2000a). However, the vertical structure of cloud fields passing the Andes could finally not be investigated due to a lack of 3D rainfall information available for the current study (TRMM-PR).

A good example for spill-over effects is given for the 22 March 1998. Heavy rainfall in the coastal plains is observed during the afternoon and early night hours (Fig. 4).

Throughout the entire day cloud patterns in the mid and upper troposphere are shifted by well developed easterlies over the Andes from the Amazon region. During late afternoon, fields of heavy precipitation form in the coastal plains and along the western Andean slopes which are associated with spill-over points and persist until midnight (Fig. 4, below). However, deep convection and resulting heavy rainfall are only observed for the western slopes by TRMM-PR 3D-data even if cold clouds are detected over both the Andes and the Amazon by GOES IR data. Because TRMM-PR is only sensitive to rain drops and not to small cloud particles, the cold clouds which are passing the Andes have been proven to be cirrus remainders from Amazon convection. They are responsible for an intensification of convection in the mid-troposphere leading to heavy precipitation in the coastal lowlands and on the western Andean slopes due to seeding effects. This mechanism is well-known in the formation of deep convection with consecutive precipitation in the Tropics (PURDOM 1995).

A completely different formation of heavy precipitation is observed on 16 March 2002 (Fig. 5).

This day is characterised by extensive rainfall over the tropical eastern Pacific (Niño 1–3 regions) which is based on MCCs. Heavy precipitation is also observed in the coastal plains of Ecuador and northern Peru (Sechura desert), but also in parts of the Ecuadorian Amazon and the eastern slopes of the Andes. The circulation pattern over the tropical eastern Pacific during this day of heavy precipitation as seen from CMWs is characterised by an anomalous westerly stream flow in the mid and higher troposphere which is typical for MCC-related situations (Fig. 5, above). However, over the Ecuadorian Amazon and the eastern Andean slopes, inverse easterly winds predominate in the mid and lower troposphere. The converging synoptic circulation patterns boost the thermal up-slope breeze systems on both sides of the Andes and thus deep convection can develop. Consequently, the TRMM-PR 3D-information points to characteristic lines of heavy precipitation ranging from the foothills up to the crests of the western and eastern cordillera (Fig. 5, below). However, no precipitation occurs in the inter-Andean basin.

4 La Niña 1999

4.1 Spatio-temporal rainfall dynamics

The spatial patterns of rainfall during the strong La Niña 1999 are nearly inverse to the situation of EN 1997/98 (Fig. 6). In general, rainfall is significantly below average in the tropical eastern Pacific sector, the coastal plains as well as the western Andean slopes. However, increased convection which is associated with heavy rainfall is observed for the Amazonian part of the study area.

For Ecuador, two areas are affected by increased precipitation: the eastern Andean slopes in the northern part over the borderline to Columbia (Quito – Ibarra – Tulcan) and the southern part in the basin of Loja as well as the area of Zamora. The central part of Ecuador reaching from the Amazon region over the Andes to the coast is relatively dry and the southern coastal part of the Sechura desert in northern Peru is completely free of rain.

The inspection of the diurnal course of rainfall reveals that deep convection in the southern part (basin of Loja) starts as early as noon (13:00 LT) and persists until 1:00 LT. In contrary to the main convective activity in the Amazon region between 13:00–19:00 LT, the north-eastern slopes of Ecuador as well as the south-eastern slopes in the area of Zamora are characterised by a second maximum of heavy rainfall during the night and the early hours of the morning (1:00–7:00 LT). From a visual inspection of satellite loops it was evident that the process of rainfall formation on the eastern Andean slopes is initiated from the Amazon basin in combination with a westward stream flow. The maximum zone of precipitation is probably associated with the valley-breeze system.

4.2 Analysis of single events

All investigated situations during La Niña 1999 reveal a strong zonal easterly flow from the Amazon to the eastern tropical Pacific in the mid and upper troposphere. Convective activity from the Amazon basin is pushed against the Andes and brings precipitation to the adjacent inter-Andean basins, especially in the

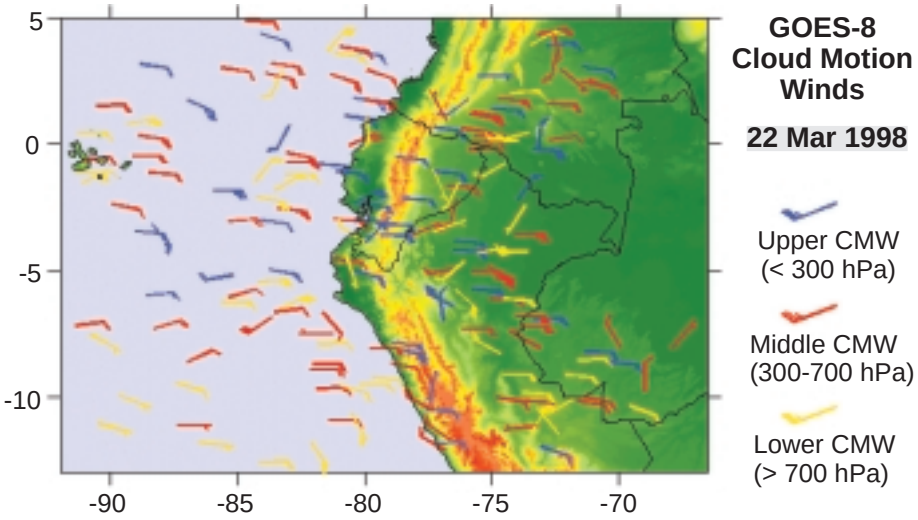

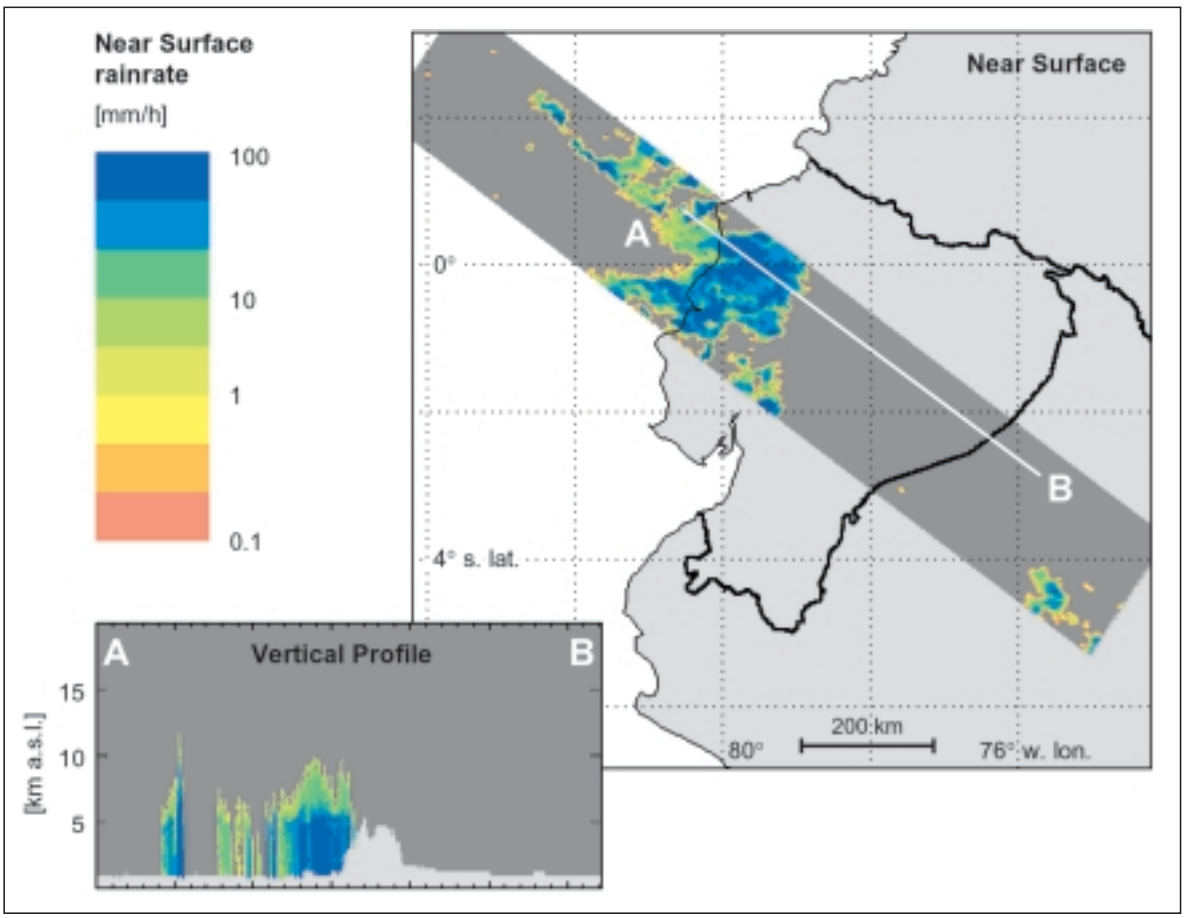

Fig. 4: Cloud Motion Winds on 22 March 1998 (13:45–14:45 LT) (above) and precipitation (TRMM-PR) at 23:32 LT (below)
Wolkenwinde für den 22. März 1998 (13:45–14:45 LT) (oben) und Niederschlag (TRMM-PR) von 23:32 LT (unten)

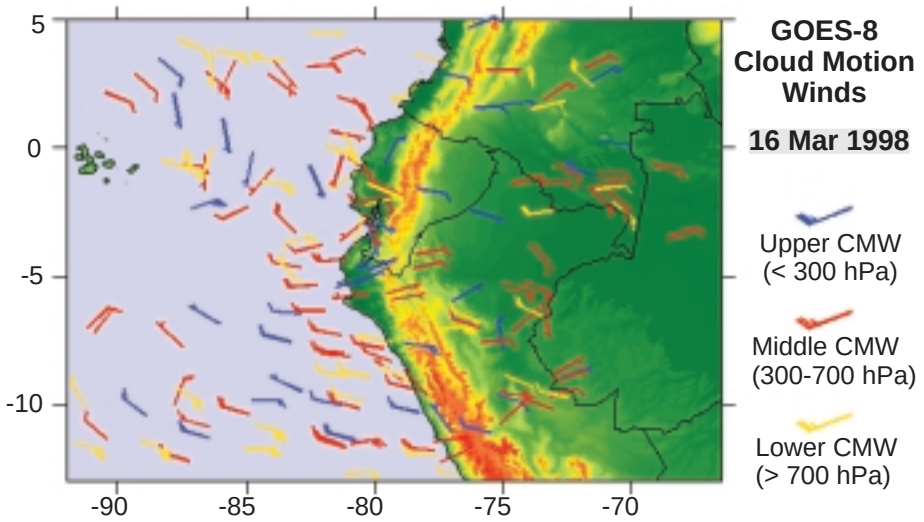

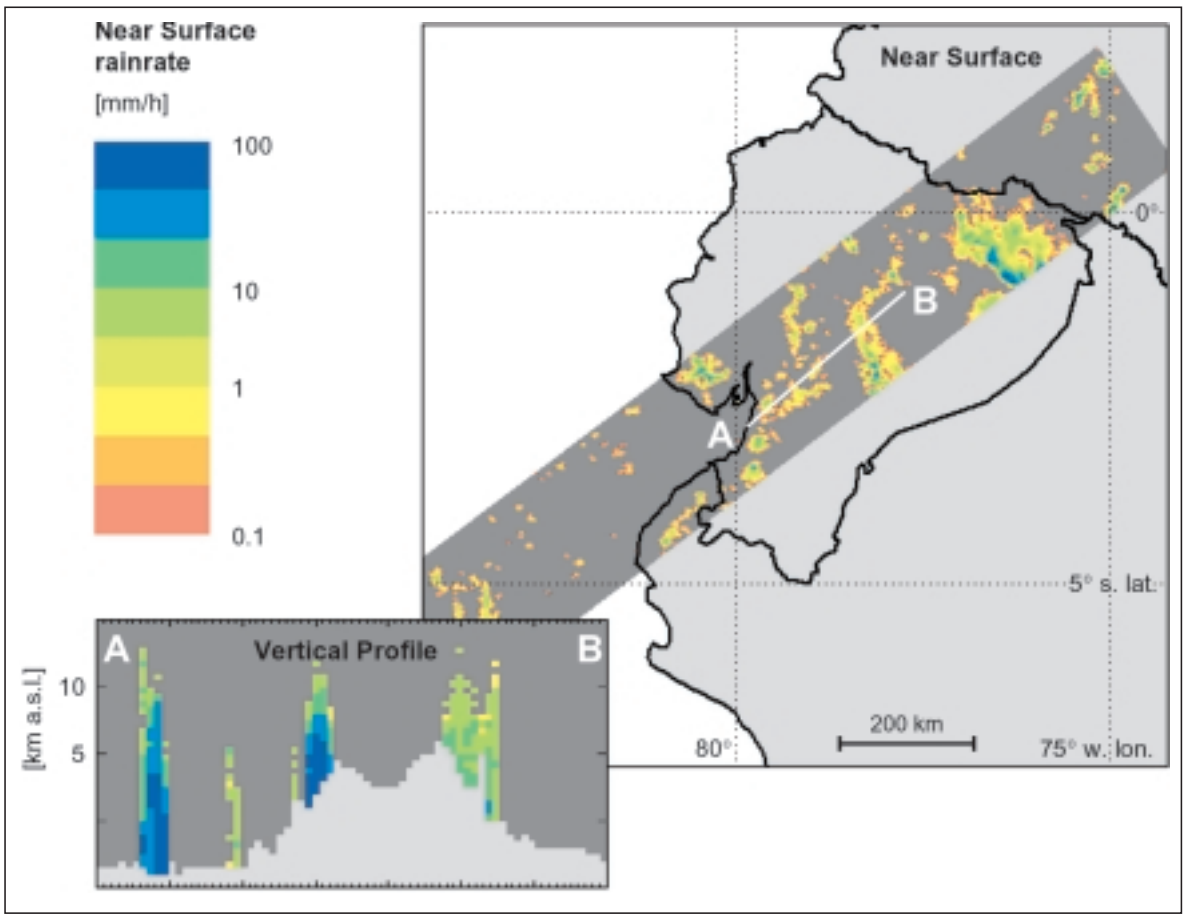

Fig. 5: Cloud Motion Winds on 16 March 1998 (14:45–15:45 LT) (above) and precipitation (TRMM-PR) at 14:30 LT (below)
Wolkenwinde für den 16. März 1998 (14:45–15:45 LT) (oben) und Niederschlag (TRMM-PR) von 14:30 LT (unten)

southern part of Ecuador where the Andes are lower as well as along east-west oriented valley systems. A typical weather situation is shown in figure 7.

The strong zonal outflows from the Amazon traverse the Andes and dominate the wind field in the upper and mid level of the troposphere over the coastal plains and the adjacent Pacific (Fig. 7). Low level winds of opposite direction are only observed by stations at the western slopes in southern Ecuador. Precipitation fields typically extend from a maximum at the Amazonian foothills up to the highlands, partially exceeding the crests of the cordillera (Fig. 7, below). If convection at the western slopes can occur, a second rainfall maximum associated with deep convection is established at the western foothills extending to higher areas.

However, if the easterly flow asserts to ground level in the coastal plain (as e. g. on 20 March 1999, Fig. 8), precipitation formation at the coast and the western Andean slopes is no longer possible due to the suppression of the coupled sea-breeze and up-slope wind phenomenon.

5 Conclusion

The current investigation by means of GOES and TRMM data has shown that the dynamics of heavy precipitation during the last Super El Niño 1997/98 is characterised by three mechanisms: (1) Rainfall formation due to mesoscale thermal systems like the land-sea-breeze phenomenon, (2) intensification of deep convection in the coastal plains by spill-over effects of cirrus remainders from the Amazon and (3) extended convection which is organised in MCCs in combination with anomalous westerly winds over the eastern Pacific. These results are in strong correspondence with previous studies of a normal El Niño 1991/92. Only the precipitation amount is much higher during the Super event in comparison to a normal EN. Precipitation dynamics during a strong La Niña (LN 1999) reveals inverse spatio-temporal patterns of deep convection and heavy rainfall formation. The coastal plains remain relatively dry whereas the eastern slopes receive above-average precipitation. Especially the strong zonal

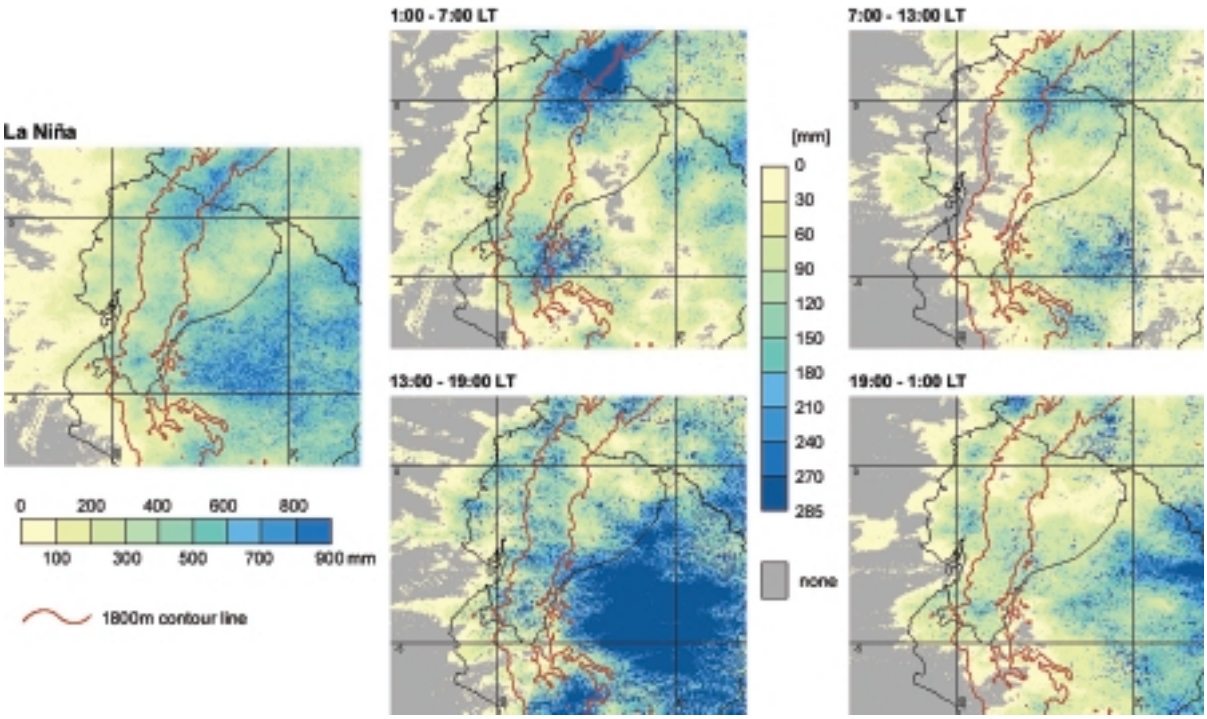

Fig. 6: Precipitation (ECST) during La Niña 1999 (10 days) (left) and diurnal course (right), LT = UTC – 5 h
Niederschlagsverteilung (ECST) während LN 1997/98 (10 Tage) (links) und Tageszeitengang (rechts), LT = UTC – 5 h

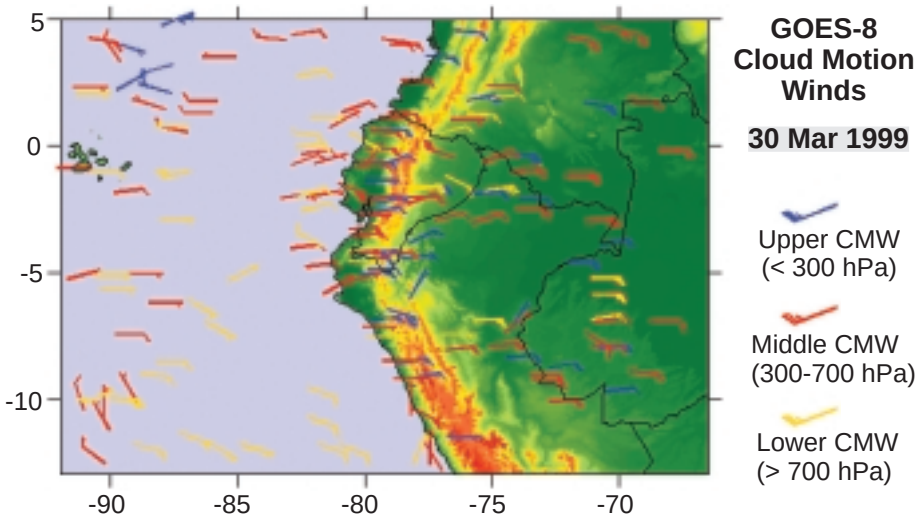

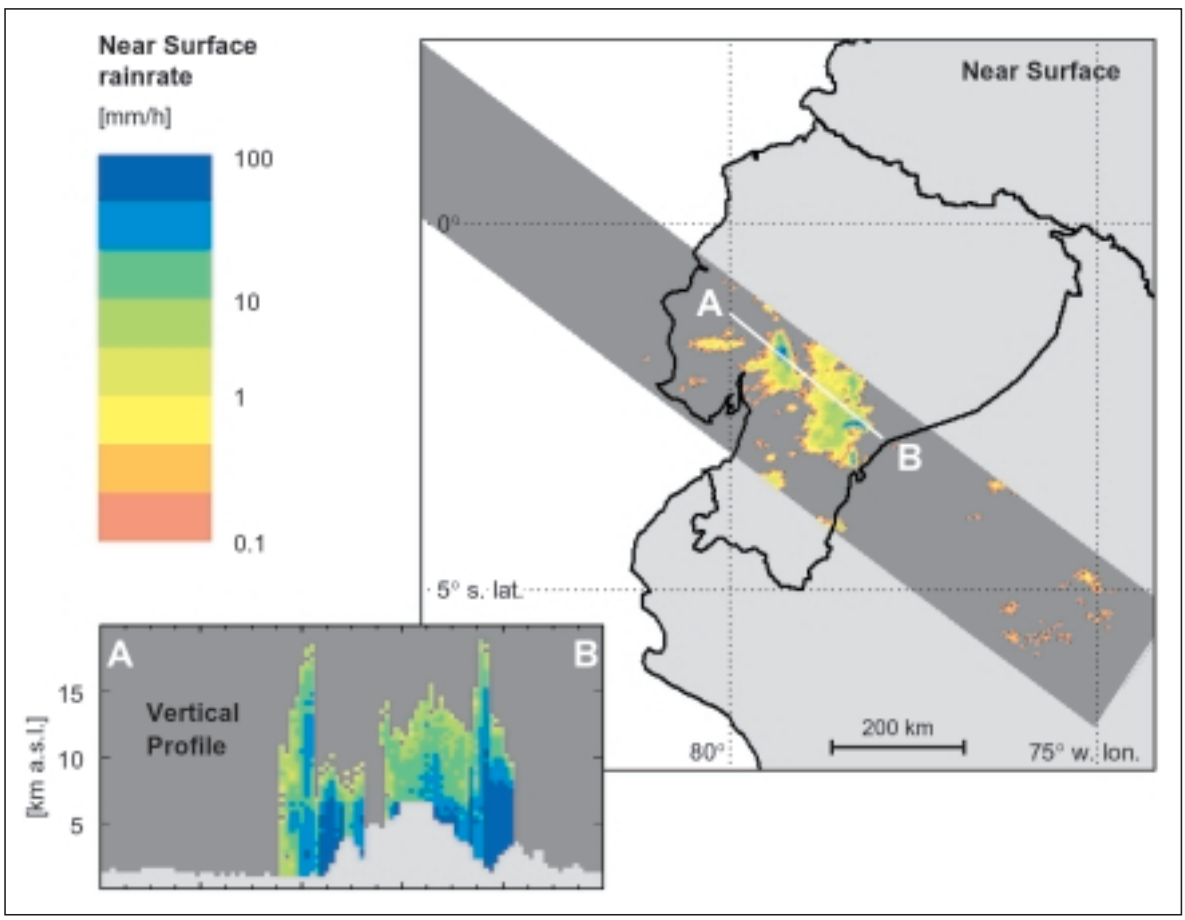

Fig. 7: Cloud Motion Winds on 30 March 1999 (13:45–14:15 LT) (above) and precipitation (TRMM-PR) at 22:49 LT (below)
Wolkenwinde für den 30. März 1999 (13:45–14:15 LT) (oben) und Niederschlag (TRMM-PR) von 22:49 LT (unten)

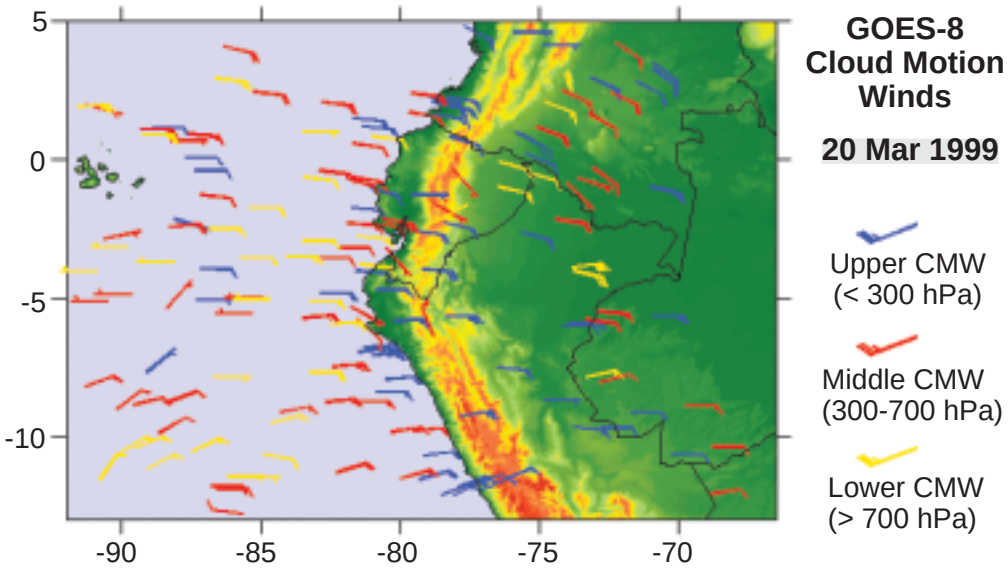

Fig. 8: Cloud Motion Winds on 20 March 1999 (12:45–13:15 LT)
Wolkenwinde für den 20. März 1999 (12:45–13:15 LT)

easterlies cause an extension of precipitation fields to the inter-Andean basins, especially in areas of the Andean depression and along east-west oriented valleys. If the easterlies can suppress the mesoscale thermal systems of the coastal plains, the coastal part of Ecuador and northern Peru remains free of rain.

References

BENDIX, J. (2000a): Precipitation dynamics in Ecuador and Northern Peru during the 1991/92 El Niño – A Remote Sensing perspective. In: Int. J. Remote Sensing 21, 533–548.

– (2000b): A comparative analysis of the major El Niño events in Ecuador and Peru over the last two decades. In: Zbl. Geol. a. Paläontol. Teil I 1999, 7/8, 1119–1131.

BENDIX, J. u. LAUER, W. (1992): Die Niederschlagsjahreszeiten in Ecuador und ihre klimadynamische Interpretation. In: Erdkunde 46, 118–134.

BENDIX, J. a. BENDIX, A. (1998): Climatological Aspects of the 1991/92 El Niño in Ecuador. In: Bulletin de L'Institut Francaise d'Etudes Andines 27, 655–666.

BENDIX, J.; BENDIX, A. u. RICHTER, M. (2000): El Niño 1997/98 in Nordperu: Anzeichen eines Ökosystem-Wandels? In: Petermanns Geogr. Mitt. 144, 20–31.

BENDIX, J. a. RAFIQPOOR, M. D. (2001): Thermal conditions of soils in the Páramo of Papallacta (Ecuador) at the upper tree line. In: Erdkunde 55, 257–276.

CAVIEDES, C. N. u. ENDLICHER, W. (1989): Die Niederschlagsverhältnisse in Nordperu während des El Niño-Southern Oscillation Ereignisses von 1983. In: Die Erde 129, 81–97.

CORNEJO, M. P. a. DE GRUNAUER, R. (2002): La Niña effects in Ecuador. www.esig.ucar.edu /lanina/report/cornejo.html

GASPARRI, E.; TASSARA, C. y VELASCO, M. (Eds.) (1999): El fenómeno de El Niño 1997–1999 en El Ecuador. Del desastre a la prevención. Ediciones Abya Yala, Quito, Ecuador, 204.

GOLDBERG, R. A.; TISNADO, M. G. a. SCOFIELD, R. A. (1987): Characteristics of extreme rainfall events in northwestern Peru during the 1982–83 El Niño period. In: J. Geophys. Res. 92, 14225–14241.

HOREL, J. D. a. CORNEJO-GARRIDO, A. G. (1986): Convection along the coast of northern Peru during 1983: spatial and temporal variation of clouds and rainfall. In: Month. Weather Rev. 114, 2091–2105.

IGUCHI, T.; KOZU, T.; MENEGHINI, R.; AWAKA, J. a. OKAMOTO, K. (2000): Rainfall-profiling algorithm for the TRMM Precipitation Radar. In: J. Appl. Meteorol. 39, 2038–2052.

KUMMEROW, C.; BARNES, W.; KOZU, T.; SHIUE, J. a. SIMPSON, J. (1998): The Tropical Rainfall Measuring Mission (TRMM) sensor package. In: J. Atmosph. Ocean Techn. 15, 809–817.

NIRALA, M. L. a. CRACKNELL, A. P. (2002): The determination of three-dimensional distribution of rain from the Tropical Rainfall Measuring Mission (TRMM) Precipitation Radar. In: Int. J. Remote Sensing 23, 4263–4304.

MCCLAIN, E. P.; PICHEL, W. G. a. WALTON, C. C. (1985): Comparative performance of AVHRR-based multichannel sea-surface temperatures. In: J. Geophys. Res. 90, 11587–11601.

MENZEL, W. P. a. PURDOM, J. F. (1994): Introducing GOES I – The first of a new generation of Geostationary Operational Environmental Satellite. In: Bul. Am. Meteorol. Soc. 75, 757–781.

PURDOM, J. F. (1995): Convective cloud pattern. In: BADER, M. J.; FORBES, G. S.; GRANT, J. R.; LILLEY, R. B. E. a. WATERS, A. J. (Eds.): Images in weather forecasting. Cambridge, 350–443.

REUDENBACH, C.; HEINEMANN, G.; HEUEL, E.; BENDIX, J. a. WINIGER, M. (2001): Investigation of summertime convective rainfall in Western Europe based on a synergy of remote sensing data and numerical models. In: Meteorology and Atmospheric Physics 76, 23–41.

ROSSEL, F.; MEJÍA, R.; ONTANEDA, G.; POMBOSA, R.; ROURA, J.; LE GOULVEN, P.; CADIER, E. et CALVEZ, R. (1998): Régionalisation de l'influence du El Niño sur les précipitations de L'Équateur. In: Bulletin de L'Institut Francaise d'Etudes Andines 27, 643–654.

SCHMETZ, J.; HOLMLUND, K.; HOFFMANN, J.; STRAUSS, B.; MASON, B.; GAERTNER, V.; KOCH, A., a. VAN DE BERG, L. (1993): Operational cloud motion winds from Meteosat infrared images. In: J. Appl. Meteorol. 32, 1206–1225.

SCHÜTTE, K. (1968): Untersuchungen zur Meteorologie und Klimatologie des El Niño-Phänomens in Ecuador und Nordperu. In: Bonner Meterol. Abh. 9. Bonn.

VAN OLDENBORGH, G. J. (2000): What caused the onset of the 1997–98 El Niño? In: Month. Weather Rev. 128, 2601–2607.

VUILLE, M.; BRADLEY, R. S. a. KEIMIG, E. (2000): Climate variability in the Andes of Ecuador and its relation to tropical Pacific and Atlantic sea surface temperature anomalies. In: J. of Climate 13, 2520–2535.

ZHOU, L.; PINKER, R. T. a. LASZLO, I. (1996): Shortwave radiative cloud forcing in the tropical Pacific including the 1982–83 and 1987 El Niños. In: Int. J. of Climatology 16, 1–13.